Ergodicity Breaking and Scaling Relations for Finite-Time First-Order Phase Transition

Yu-Xin Wu,[1] Jin-Fu Chen,[1,2,*] and H. T. Quan[1,3,4,†]
[1]School of Physics, Peking University, Beijing 100871, China
[2]Instituut-Lorentz, Universiteit Leiden, P.O. Box 9506, 2300 RA Leiden, The Netherlands
[3]Collaborative Innovation Center of Quantum Matter, Beijing 100871, China
[4]Frontiers Science Center for Nano-Optoelectronics, Peking University, Beijing 100871, China

(Received 10 July 2024; accepted 3 April 2025; published 2 May 2025)

Hysteresis and metastable states are typical features associated with ergodicity breaking in the first-order phase transition. We explore the scaling relations of nonequilibrium thermodynamics in finite-time first-order phase transitions. Using the Curie-Weiss model as an example, for large systems we find the excess work scales as $v^{2/3}$ when the magnetic field is quenched at a finite rate v across the phase transition. We further reveal a crossover in the scaling of the excess work from $v^{2/3}$ to v when downsizing the system. Our study elucidates the interplay between the finite-time dynamics and the finite-size effect, which leads to different scaling behaviors of the excess work with or without ergodicity breaking.

DOI: 10.1103/PhysRevLett.134.177101

Introduction—Phase transitions are drastic changes of a system's state under variation of the external parameters [1,2]—for example, the density in a temperature-driven liquid-gas transition, or the magnetization in a paramagnet-ferromagnet transition [3]. In the past few decades, owing to the recent development of nonequilibrium thermodynamics [4–11], there is a growing interest in the field of stochastic thermodynamics with phase transitions [12–27]. A central concept in thermodynamics is the work performed on such a system [28–34], when some external parameters of the system are varied with time. The second law of thermodynamics constrains that the work W performed on the system is no less than the free energy difference ΔF between the initial and final states. In other words, the excess work done in a finite-rate quench with respect to the quasistatic quench process is non-negative $W - \Delta F \geq 0$. A natural question is how thermodynamic quantities such as the excess work scale with the rate of quench.

In the regular cases without phase transition, it is well-known that in slow isothermal processes, the excess work is proportional to the quench rate as a result of the linear response theory [35–46]. While in slow adiabatic processes, the excess work is proportional to the square of the quench rate according to the adiabatic perturbation theory [47–52]. In the presence of phase transitions, the scaling behavior becomes much more involved. For the second-order phase transition, it is found that the excess work done during a quench across the critical point exhibits power-law behavior with the quench rate, and the corresponding exponents are fully determined by the dimension of the system and the critical exponents of the transition [22,53], as in the traditional Kibble-Zurek mechanism [54–59]. Besides the second-order phase transition, the first-order phase transition is ubiquitous in nature, e.g., in biochemical [10,17,25,60,61], ecological [62], and electronic systems. Such phase transitions have been studied in the past three decades [63–71], mainly focusing on dynamical properties in the thermodynamic limit with ergodicity breaking [72]. However, the stochastic thermodynamics of the first-order phase transition remains largely unexplored. Also, a central problem in statistical mechanics is how the finite-size effect will influence the thermodynamic properties. For mesoscopic systems, nevertheless, little is known about how the finite-size effect influences the thermodynamic properties of finite-time first-order phase transitions.

In this Letter, we study the ergodicity breaking [72] and the scaling behavior of the excess work with the quench rate v in the first-order phase transition. Our focus is put on the interplay between the finite time of the quench process and the finite size of the system. Using the Curie-Weiss model with a varying magnetic field as a paradigmatic example [26,73,74], we find the $v^{2/3}$ scaling relation of the excess work with the quench rate for a large system. The delay time and the transition time are found to scale as $v^{-1/3}$. When downsizing the system, ergodicity of the system is restored, and the hysteresis shrinks. Meanwhile, the scaling of the excess work transitions from $v^{2/3}$ to v. These results will be helpful in optimizing the energy cost and the speed of thermodynamic processes, and may have potential applications in information erasure and heat-engine design.

The model—We consider the kinetic Curie-Weiss model with ferromagnetic interaction introduced in Refs. [26,75].

*Contact author: jinfuchen@lorentz.leidenuniv.nl
†Contact author: htquan@pku.edu.cn

The Curie-Weiss model consists of N Ising spins $\sigma_i = \pm 1$, labeled $i = 1, \dots, N$, with the coupling strength $J/(2N)$. The system is embedded in a heat reservoir at an inverse temperature $\beta = 1/(k_B T)$, and subject to a varying field $H(t)$ controlled by some external agent. The state of the system can be characterized by the magnetic moment $M = \sum_i \sigma_i$. A single spin can flip $\pm 1 \to \mp 1$ due to thermal fluctuations of the heat bath, and the magnetic moment changes as $M \to M_\pm = M \pm 2$. The probability $P(M,t)$ of finding the system in state M at time t evolves under the master equation,

$$\frac{\partial P(M,t)}{\partial t} = \sum_{\eta=\pm} [W_\eta(M_{-\eta}, H(t)) P(M_{-\eta}, t) - W_\eta(M, H(t)) P(M,t)]. \quad (1)$$

The corresponding transition rates $W_\pm(M,H)$ under the external field H are given by [75]

$$W_\pm(M,H) = \frac{N \mp M}{2\tau_0} e^{\pm\beta[J(M\pm1)/N + H]}, \quad (2)$$

with microscopic relaxation time τ_0.

In the thermodynamic limit $N \to \infty$, we use the mean magnetization $m \equiv M/N$ to denote the system state. The internal energy density is given by

$$\mathcal{H}(m,H) = -\frac{J}{2} m^2 - Hm. \quad (3)$$

The deterministic dynamics is described by the equation of motion of $m(t)$ [26,76],

$$\frac{dm}{dt} = \frac{2}{\tau_0}[\sinh(\beta J m + \beta H) - m\cosh(\beta J m + \beta H)] \equiv f(m,H), \quad (4)$$

with the microscopic relaxation time τ_0.

The curve characterizing steady state as a function of H is shown in Fig. 1, where we choose the parameters to be $\tau_0 = 2$, $J = 1$, $\beta = 2$. For different H, the ordinary differential equation (4) can have one, two, or three steady-state solutions. For small and large values of H, the system has only one steady state, i.e., the system is monostable. For intermediate values of H, there are three steady states: m_{top}, m_{bot}, and m_{mid}, i.e., the system exhibits bistability. Among the three, one is globally stable; one is metastable, and the one in between is unstable. The two black dots are the turning points $(H_\pm, m_\pm)$, where the metastability disappears.

During the quench process, the external field H is tuned quasistatically from $H_i = -1.0$ to $H_f = 1.0$. The quasistatic hysteresis loop is shown with the pink dotted curve in Fig. 1. The quasistatic state m_{qs} gets trapped in the local minimum as H is increased quasistatically from H_i to H_f, i.e., m_{qs} follows the lower branch m_{bot} even when the local minimum is metastable rather than globally stable, until the right turning point (H_+, m_+). Then the system state jumps to the upper branch. This is what we refer to as "quasistatic first-order phase transition." So much the same for the return path. The quasistatic state m_{qs} remains on the upper branch and jumps down to the lower branch at the left turning point (H_-, m_-).

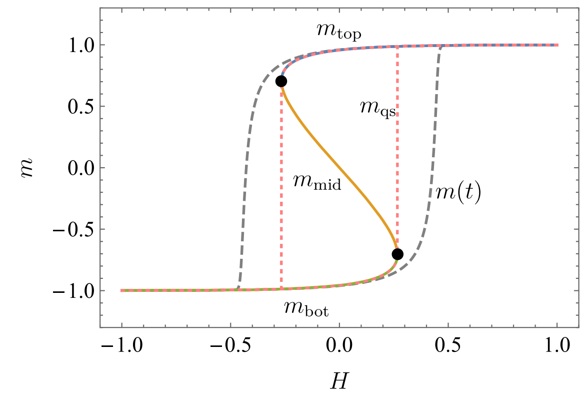

FIG. 1. Quasistatic and dynamic hysteresis loops for Curie-Weiss model. The top, middle, and bottom solid lines show the steady states m_{top}, m_{mid}, and m_{bot} as functions of H. The black dots denote the right and left turning points $(H_\pm, m_\pm)$. The pink dotted lines indicate the quasistatic state m_{qs}. The gray dashed lines represent the transient state of the system $m(t)$ when H is quenched at the rate $v = 6$.

When $H(t)$ is tuned at a finite rate v, the system tries to keep pace with—but ultimately lags behind—the continually changing quasistatic state, as is shown by the gray dashed curve in Fig. 1. This mismatch becomes evident around the turning point. A detailed illustration of the finite-time first-order phase transition can be found in [76].

Scaling relations of time—During the quench process, the trajectory follows local equilibrium, be it metastable or globally stable, until an abrupt transition into a totally different state from the original one. This transition relies on the system's history and is regarded as a finite-time first-order phase transition. This is caused by the collapse of the metastable state. The turning points $(H_\pm, m_\pm) = (\pm H^*, \pm m^*)$ are solved from $f(m,H) = 0$ and $\partial_m f(m,H) = 0$ as

$$m^* = -\sqrt{1 - \frac{1}{\beta J}}, \quad (5)$$

$$H^* = \frac{1}{\beta}\left[\sqrt{\beta J(\beta J - 1)} - \operatorname{arctanh}\left(\sqrt{\frac{\beta J - 1}{\beta J}}\right)\right]. \quad (6)$$

We consider the case in which the external magnetic field $H(t)$ is varied from the initial value H_i to the final value H_f

according to the linear protocol

$$H(t) = H_i + (H_f - H_i)\frac{t}{t_f}, \qquad 0 \le t \le t_f, \tag{7}$$

with the quench rate $v = (H_f - H_i)/t_f$ and the time duration t_f. We label the time when $H(t)$ reaches the right turning point H^* as the turning time t^* [62].

It is important to note that while the potential landscape has drastically changed from bistable to monostable at the turning time t^*, in a finite-rate quench the dynamics of the system cannot catch up with the change of the potential landscape, i.e., the system displays a delay in transitioning to the global minimum. The transition occurs later than the turning time t^* by a delay time $\hat{t}_{\rm del}$ defined through $m(t^* + \hat{t}_{\rm del}) = m^*$. The delay time depends on the quench rate v.

We further analyze the scaling relation between the delay time and the quench rate. We shift the variables in the following way: $\hat{H} = H - H^*$, $\hat{m} = m - m^*$, $\hat{t} = t - t^*$. The evolution equation is turned into

$$\begin{aligned}\frac{d\hat{m}}{d\hat{t}} &= f(m^* + \hat{m}, H^* + v\hat{t})\\ &\approx \frac{2}{\tau_0}\left[\beta J\sqrt{\beta J - 1}\hat{m}^2 + \sqrt{\frac{\beta}{J}}v\hat{t}\right].\end{aligned} \tag{8}$$

In the second line, the equation of motion is expanded around the turning point for slow quench approximation [76]. It can be adimensionalized into [80]

$$\frac{du}{ds} = u^2 + s \tag{9}$$

by rescaling the variables $u = \alpha\hat{m}$, $s = \gamma\hat{t}$, where $\alpha = (\beta J\sqrt{\beta J - 1})^{2/3}(\tau_0 v\sqrt{\beta/J}/2)^{-1/3}$ and $\gamma = (\beta J\sqrt{\beta J - 1})^{1/3}(4v\sqrt{\beta/J}/\tau_0^2)^{1/3}$.

Under the asymptotic boundary condition $s \to -\infty$, $u \to \sqrt{-s}$, the solution to Eq. (9) is the Airy function [63]

$$u(s) = \frac{\mathrm{Ai}'(-s)}{\mathrm{Ai}(-s)}. \tag{10}$$

In this way, the delay time can be computed as

$$\hat{t}_{\rm del} = -A_1'\left[4\sqrt{\beta J(\beta J - 1)}\frac{\beta}{\tau_0^2}v\right]^{-1/3}, \tag{11}$$

where $A_1' \approx -1.019$ represents the first zero point of the Airy prime function.

Besides the delay time $\hat{t}_{\rm del}$, there is another time $\hat{t}_{\rm trans}$ characterizing the non-catching-up of the dynamics. When the system is quenched at a finite rate, the transition time $\hat{t}_{\rm trans}$ to reach the monostable state, which is defined through $m(t^* + \hat{t}_{\rm trans}) = m_{\rm nd}$, depends on the quench rate v. Here $m_{\rm nd} \approx 1 + 2e^{-2\beta J - 2\sqrt{\beta J(\beta J - 1)}}/(2\sqrt{\beta J(\beta J - 1)} - 2\beta J + 1)$ stands for the nondegenerate root of $f(m, H_+) = 0$. For $\beta J \gg 1$, $m_{\rm nd}$ can be approximated by 1. The transition time can be calculated as

$$\hat{t}_{\rm trans} = -A_1\left[4\sqrt{\beta J(\beta J - 1)}\frac{\beta}{\tau_0^2}v\right]^{-1/3}, \tag{12}$$

where $A_1 \approx -2.338$ stands for the first zero point of the Airy function [62].

Equations (11) and (12) show that both the delay time and the transition time scale with the quench rate as $v^{-1/3}$. The matching between analytical expressions and numerical results for $\hat{t}_{\rm del}$ and $\hat{t}_{\rm trans}$ is presented in Fig. 2. The exponent $-1/3$ results from the quadratic leading order $\hat{m}^2$ in Eq. (8) around the turning point.

Scaling relation of excess work for large systems—In a finite-rate quench process, the work performed on the system is greater than that in the quasistatic quench process. In other words, the non-catching-up in the dynamics between the transient state and the quasistatic state results in the excess work, which characterizes the irreversibility of the process. It is desirable to explore the relation between the excess work and the quench rate.

From the microscopic definition of work [86,87], the work (per site) performed on the system is

$$w = \int_0^{t_f} dt \frac{\partial \mathcal{H}}{\partial H}\dot{H} = -v\int_0^{t_f} dt m(t). \tag{13}$$

In the quasistatic isothermal process, the work can be calculated from

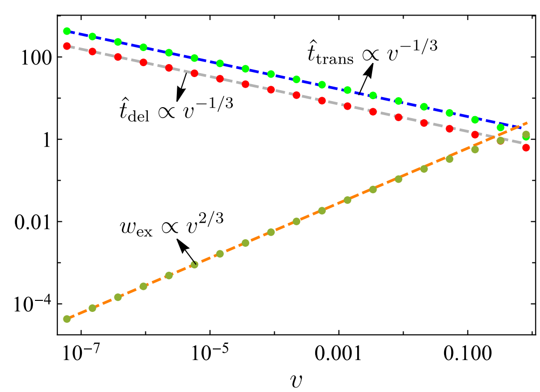

FIG. 2. The scaling relations of the delay time, the transition time, and the excess work with the quench rate. The delay time $\hat{t}_{\rm del}$ and the transition time $\hat{t}_{\rm trans}$ scale as $v^{-1/3}$ while the excess work scales as $v^{2/3}$. The dots are obtained by numerically solving Eqs. (4) and (13). The dashed lines show the analytical expressions in Eqs. (11), (12), and (15).

$$w_{\text{qs}} = \int_{H_i}^{H_f} dH \frac{\partial \mathcal{H}(m_{\text{qs}}, H)}{\partial H}. \tag{14}$$

The excess work, defined as $w_{\text{ex}} = w - w_{\text{qs}}$, describes the excess amount work that one has to perform when the system is quenched at a finite rate rather than quasistatically. In a slow quench, the excess work can be approximated by the enclosed rectangular area between the dynamic and quasistatic hysteresis (see Fig. 1),

$$\begin{aligned} w_{\text{ex}} &\approx v\hat{t}_{\text{trans}}(m_{\text{nd}} - m^*) \\ &\approx \frac{-A_1\left(1+\sqrt{1-\frac{1}{\beta J}}\right)}{\left[4\sqrt{\beta J(\beta J-1)}\frac{\beta}{\tau_0^2}\right]^{1/3}} v^{2/3}, \end{aligned} \tag{15}$$

where we approximate m_{nd} with 1 in the second line. Equation (15) shows that the excess work scales with the quench rate as $w_{\text{ex}} \propto v^{2/3}$, which is verified numerically in Fig. 2. This $2/3$ scaling relation of the excess work is due to the breaking of ergodicity [72] in large systems.

Scaling relation of excess work for small systems—So far, the results above are caused by neglecting the fluctuations that disappear for infinitely large systems. Nevertheless, for small systems, fluctuations become non-negligible. A central problem in statistical mechanics is how the finite-size effect will influence the thermodynamic properties. We further study the scaling relation of excess work for small systems.

In order to take fluctuations into consideration, a stochastic approach has to be envisaged. For finite systems, M is a random variable, and its probability distribution $P(M,t)$ evolves under the master equation (1). The average magnetization per site $\langle m \rangle = \sum_M MP(M,t)/N$ can be calculated from the solution of the master equation (1). Figure 3(a) shows the mean magnetization for finite-size systems. The dynamic hysteresis loop approaches the deterministic case (dashed gray curve) as the system size N increases, and shrinks as N decreases.

The work done on a system during the manipulation of the external field, along a stochastic trajectory $m(t)$, is given by Eq. (13). The average work can be calculated from

$$\langle w \rangle = -v \int_0^{t_f} dt \langle m(t) \rangle. \tag{16}$$

The average excess work is defined as the average total work subtracted by the quasistatic work $\langle w_{\text{ex}} \rangle = \langle w \rangle - w_{\text{qs}}$.

For small systems, in the slow driving regime, the quench rate is slower than the system's relaxation rate, which depends on the system size. The system is ergodic and the dynamics falls within the near-equilibrium regime without phase transition. The quasistatic work is equal to the free energy difference that vanishes when $H_f = -H_i$ (due to the symmetry of Curie-Weiss model). Thus, the

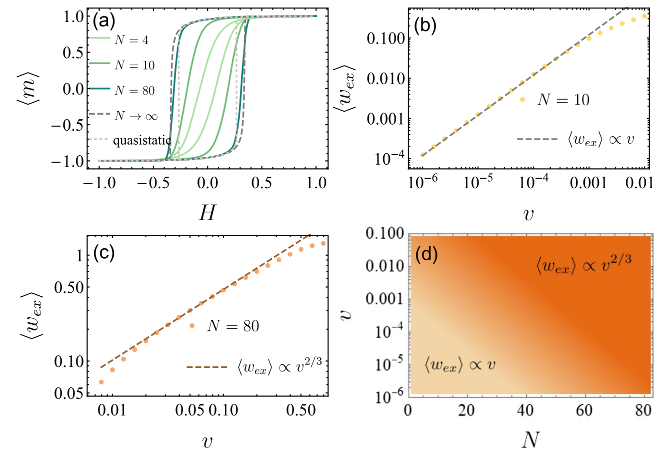

FIG. 3. The finite-size effect on the dynamic and thermodynamic properties. (a) The hysteresis loop: the average magnetization per site $\langle m \rangle$ as a function of the magnetic field H for different system sizes N. The green solid lines represent the cases for $N = 4, 10, 80$ from the inside out. The dashed and dotted line, respectively, represent the dynamic and static hysteresis with $N \to \infty$. The quench rate is fixed at the same value $v = 0.01$ for all curves. (b) For $N = 10$. the average excess work is proportional to the quench rate as $\langle w_{\text{ex}} \rangle \propto v$. (c) For $N = 80$, the average excess work scales as $\langle w_{\text{ex}} \rangle \propto v^{2/3}$. The dots in (b) and (c) are obtained from numerically solving Eqs. (1) and (16). (d) The crossover between two regimes in the N–v plane. The excess work scales as $\langle w_{\text{ex}} \rangle \propto v$ in the light-color region, and $\langle w_{\text{ex}} \rangle \propto v^{2/3}$ in the dark-color region (see [76] for details).

excess work equals the total work, which is proportional to the quench rate v, i.e., $\langle w_{\text{ex}} \rangle \sim v$ [see Fig. 3(b)] as a consequence of the linear response theory [35–46].

For large systems, when the quench rate is slow but not slower than the system's relaxation rate, nonergodic behavior emerges and the quasistatic work can be approximated by that in the deterministic limit. We plot the average excess work $\langle w_{\text{ex}} \rangle$ as a function of the quench rate v for system size $N = 80$ in Fig. 3(c). We observe that the average excess work scales as $\langle w_{\text{ex}} \rangle \propto v^{2/3}$ when the quench rate is slow but not too slow. As the quench further slows down, ergodicity is gradually restored, leading to the deviation from the $2/3$ scaling.

As the system size increases, the scaling of the average excess work transitions from $\langle w_{\text{ex}} \rangle \propto v$ to $\langle w_{\text{ex}} \rangle \propto v^{2/3}$ [see Fig. 3(d) and [76] for details]. This crossover is a consequence of the breaking of ergodicity [72], which has its origin in the interplay between the quench rate and the relaxation rate (system size). For small N, thermal fluctuation is strong enough to overcome the energy barrier between two minima. The system is ergodic and the linear scaling relation $\langle w_{\text{ex}} \rangle \propto v$ can be explained with the linear response theory. As the system size increases, the first-order phase transition shows up. For large N, thermal fluctuation cannot overcome the energy barrier, and ergodicity is broken [72], leading to the $2/3$ scaling of the

TABLE I. The scaling relations of the excess work w_{ex} with the quench rate v for different situations.

Finite-time isothermal process [35–46]	$w_{ex} \propto v$
Finite-time adiabatic process [47–52]	$w_{ex} \propto v^2$
Finite-time first-order phase transition	$w_{ex} \propto v^{2/3}$
Finite-time second-order phase transition [22,53]	$w_{ex} \propto v^{\delta_1}$

excess work. Moreover, it is noteworthy that stochastic thermodynamics brings us more information apart from the average value of work. By evaluating the probability distribution of work for finite-size system, Jarzynski's equality is verified [76].

Last but not least, we would like to compare our results in the first-order phase transition for open systems with those in the second-order phase transition for isolated quantum systems and the cases without phase transition in Table I. In the second-order phase transition for isolated quantum systems, the v^{δ_1} scaling behavior of the excess work due to finite-rate quench is obtained for isolated quantum systems in Refs. [22,53]. It is relevant to but different from the Kibble-Zurek scaling for the average density of defects [54–57]. The scaling exponent δ_1 is determined by the dimension of the system and the critical exponents of the transition. While the v^{δ_1} scaling behavior is valid for large systems, it transitions [22] to v^2 for small systems without phase transition according to the adiabatic perturbation theorem [47–52]. In the first-order phase transition for open systems, we find that the excess work scales as $v^{2/3}$ for large systems where ergodicity is broken [65,66,68–72]. When downsizing the system, there is a crossover in the scaling relation of the excess work from $v^{2/3}$ to v. In small systems where ergodicity is restored, the scaling relation transitions to $w_{ex} \propto v$ in finite-time isothermal processes without phase transition, as a result of linear response theory [35–46].

Conclusions—In this Letter, we study the excess work in a finite-time first-order phase transition. We show a $v^{2/3}$ scaling relation of the excess work, which manifests itself as a sign of ergodicity breaking [72] in large systems, and its crossover to v when downsizing the system. The underlying mechanism of such a crossover is that ergodicity is restored when decreasing the system size. The hysteresis and metastable state disappear in small systems, and the scaling behavior of the excess work transitions to the case without phase transition. It can be seen that in order to minimize the energy dissipation, one should avoid ergodicity breaking. Our results on the crossover in the scaling relation between excess work and quench rate in first-order phase transitions of finite-size systems enhance the understanding of finite-time phase transitions and nonequilibrium thermodynamics in driven systems, with potential applications in information erasure and heat-engine design. Our findings have general relevance beyond the present model, extending to various systems undergoing the first-order phase transitions [76], including open quantum systems [81–83] and chemical reaction networks [25,84,85]. In the future, it is desirable to explore the scaling properties of the higher moments of the excess work [22] and the scaling properties of quantum first-order phase transitions, which would hopefully bring more insights about the nonequilibrium properties of phase transitions.

Acknowledgments—The authors acknowledge helpful discussions with Wei-Mou Zheng. This work is supported by the National Natural Science Foundations of China (NSFC) under Grants No. 12375028, No. 11825501, and No. 12147157.

[1] H. B. Callen, *Thermodynamics and an Introduction to Thermostatistics* (John Wiley and Sons, New York, 1985).

[2] N. Goldenfeld, *Lectures on Phase Transitions and the Renormalization Group* (CRC Press, Boca Raton, 1992).

[3] P. M. Chaikin and T. C. Lubensky, *Principles of Condensed Matter Physics* (Cambridge University Press, Cambridge, England, 1995), Vol. 10.

[4] R. Graham and T. Tél, Phys. Rev. Lett. **52**, 9 (1984).

[5] J. Keizer, *Statistical Thermodynamics of Nonequilibrium Processes* (Springer, New York, New York, 1987).

[6] A. Imparato and L. Peliti, C.R. Phys. **8**, 556 (2007).

[7] U. Seifert, Rep. Prog. Phys. **75**, 126001 (2012).

[8] T. Sagawa, J. Stat. Mech. (2014) P03025.

[9] L. Bertini, A. De Sole, D. Gabrielli, G. Jona-Lasinio, and C. Landim, Rev. Mod. Phys. **87**, 593 (2015).

[10] M. Pineda and M. Stamatakis, Entropy **20**, 811 (2018).

[11] L. Peliti and S. Pigolotti, *Stochastic Thermodynamics* (Princeton University Press, Princeton, 2021).

[12] B. Derrida, J. Phys. A **20**, L721 (1987).

[13] J. P. Garrahan, R. L. Jack, V. Lecomte, E. Pitard, K. van Duijvendijk, and F. van Wijland, Phys. Rev. Lett. **98**, 195702 (2007).

[14] J. Mehl, T. Speck, and U. Seifert, Phys. Rev. E **78**, 011123 (2008).

[15] D. Lacoste, A. W. C. Lau, and K. Mallick, Phys. Rev. E **78**, 011915 (2008).

[16] R. L. Jack and P. Sollich, Prog. Theor. Phys. Suppl. **184**, 304 (2010).

[17] H. Ge and H. Qian, J. R. Soc. Interface **8**, 107 (2010).

[18] T. Herpich, J. Thingna, and M. Esposito, Phys. Rev. X **8**, 031056 (2018).

[19] P. T. Nyawo and H. Touchette, Phys. Rev. E **98**, 052103 (2018).

[20] T. A. Byrd, A. Erez, R. M. Vogel, C. Peterson, M. Vennettilli, G. Altan-Bonnet, and A. Mugler, Phys. Rev. E **100**, 022415 (2019).

[21] C. E. Fernández Noa, P. E. Harunari, M. J. de Oliveira, and C. E. Fiore, Phys. Rev. E **100**, 012104 (2019).

[22] Z. Fei, N. Freitas, V. Cavina, H. T. Quan, and M. Esposito, Phys. Rev. Lett. **124**, 170603 (2020).

[23] H. Vroylandt, M. Esposito, and G. Verley, Phys. Rev. Lett. **124**, 250603 (2020).

[24] K. Proesmans, R. Toral, and C. Van den Broeck, Physica (Amsterdam) **552A**, 121934 (2020).
[25] B. Nguyen and U. Seifert, Phys. Rev. E **102**, 022101 (2020).
[26] J. Meibohm and M. Esposito, Phys. Rev. Lett. **128**, 110603 (2022).
[27] N. Freitas, K. Proesmans, and M. Esposito, Phys. Rev. E **105**, 034107 (2022).
[28] T. Speck and U. Seifert, Phys. Rev. E **70**, 066112 (2004).
[29] T. Speck and U. Seifert, Eur. Phys. J. B **43**, 521 (2005).
[30] V. Blickle, T. Speck, L. Helden, U. Seifert, and C. Bechinger, Phys. Rev. Lett. **96**, 070603 (2006).
[31] H. T. Quan, S. Yang, and C. P. Sun, Phys. Rev. E **78**, 021116 (2008).
[32] A. Engel, Phys. Rev. E **80**, 021120 (2009).
[33] D. Nickelsen and A. Engel, Eur. Phys. J. B **82**, 207 (2011).
[34] A. Ryabov, M. Dierl, P. Chvosta, M. Einax, and P. Maass, J. Phys. A **46**, 075002 (2013).
[35] P. Salamon, A. Nitzan, B. Andresen, and R. S. Berry, Phys. Rev. A **21**, 2115 (1980).
[36] P. Salamon and R. S. Berry, Phys. Rev. Lett. **51**, 1127 (1983).
[37] O. Mazonka and C. Jarzynski, arXiv:cond-mat/9912121.
[38] T. Schmiedl and U. Seifert, Europhys. Lett. **81**, 20003 (2007).
[39] G. E. Crooks, Phys. Rev. Lett. **99**, 100602 (2007).
[40] M. Esposito, R. Kawai, K. Lindenberg, and C. Van den Broeck, Phys. Rev. Lett. **105**, 150603 (2010).
[41] Z. Gong, Y. Lan, and H. T. Quan, Phys. Rev. Lett. **117**, 180603 (2016).
[42] V. Cavina, A. Mari, and V. Giovannetti, Phys. Rev. Lett. **119**, 050601 (2017).
[43] Y.-H. Ma, D. Xu, H. Dong, and C.-P. Sun, Phys. Rev. E **98**, 022133 (2018).
[44] M. Scandi and M. Perarnau-Llobet, Quantum **3**, 197 (2019).
[45] Y.-H. Ma, R.-X. Zhai, J. Chen, C. P. Sun, and H. Dong, Phys. Rev. Lett. **125**, 210601 (2020).
[46] J.-F. Chen, C. P. Sun, and H. Dong, Phys. Rev. E **104**, 034117 (2021).
[47] C.-P. Sun, J. Phys. A **21**, 1595 (1988).
[48] A. Polkovnikov, Phys. Rev. B **72**, 161201(R) (2005).
[49] G. Rigolin, G. Ortiz, and V. H. Ponce, Phys. Rev. A **78**, 052508 (2008).
[50] C. De Grandi and A. Polkovnikov, *Quantum Quenching, Annealing and Computation* (Springer Berlin Heidelberg, Heidelberg, 2010), pp. 75–114.
[51] A. Polkovnikov, K. Sengupta, A. Silva, and M. Vengalattore, Rev. Mod. Phys. **83**, 863 (2011).
[52] J.-F. Chen, C.-P. Sun, and H. Dong, Phys. Rev. E **100**, 062140 (2019).
[53] F. Zhang and H. T. Quan, Phys. Rev. E **105**, 024101 (2022).
[54] T. W. B. Kibble, J. Phys. A **9**, 1387 (1976).
[55] T. Kibble, Phys. Rep. **67**, 183 (1980).
[56] W. H. Zurek, Nature (London) **317**, 505 (1985).
[57] W. Zurek, Phys. Rep. **276**, 177 (1996).
[58] A. del Campo, Phys. Rev. Lett. **121**, 200601 (2018).
[59] J.-M. Cui, F. J. Gómez-Ruiz, Y.-F. Huang, C.-F. Li, G.-C. Guo, and A. del Campo, Commun. Phys. **3**, 44 (2020).
[60] H. Ge and H. Qian, Phys. Rev. Lett. **103**, 148103 (2009).
[61] H. Qian, P. Ao, Y. Tu, and J. Wang, Chem. Phys. Lett. **665**, 153 (2016).
[62] J. H. Li, F. X.-F. Ye, H. Qian, and S. Huang, J. Phys. D **395**, 7 (2019).
[63] P. Jung, G. Gray, R. Roy, and P. Mandel, Phys. Rev. Lett. **65**, 1873 (1990).
[64] F. Zhong, J. X. Zhang, and G. G. Siu, J. Phys. Condens. Matter **6**, 7785 (1994).
[65] A. Hohl, H. J. C. van der Linden, R. Roy, G. Goldsztein, F. Broner, and S. H. Strogatz, Phys. Rev. Lett. **74**, 2220 (1995).
[66] G. P. Zheng and J. X. Zhang, J. Phys. Condens. Matter **10**, 1863 (1998).
[67] B. K. Chakrabarti and M. Acharyya, Rev. Mod. Phys. **71**, 847 (1999).
[68] N. Berglund and H. Kunz, J. Phys. A **32**, 15 (1999).
[69] F. Zhong, Front. Phys. **12**, 126402 (2017).
[70] S. Scopa and S. Wald, J. Stat. Mech. (2018) 113205.
[71] S. Kundu, R. K. Patel, S. Middey, and B. Bansal, Phys. Rev. E **108**, 024101 (2023).
[72] R. G. Palmer, Adv. Phys. **31**, 669 (1982).
[73] R. Fernández, F. den Hollander, and J. Martínez, Commun. Math. Phys. **319**, 703 (2012).
[74] F. Collet and M. Formentin, J. Stat. Phys. **176**, 478 (2019).
[75] J. Meibohm and M. Esposito, New J. Phys. **25**, 023034 (2023).
[76] See Supplemental Material at http://link.aps.org/supplemental/10.1103/PhysRevLett.134.177101 for details of derivations and calculations, which includes Refs. [77–79].
[77] A. Imparato and L. Peliti, Europhys. Lett. **70**, 740 (2005).
[78] A. Imparato and L. Peliti, Phys. Rev. E **72**, 046114 (2005).
[79] K. Matsuo, J. Stat. Phys. **16**, 169 (1977).
[80] To demonstrate the generality of the rescaled dynamics in Eq. (9) for finite-time first-order phase transitions, we derive the same effective equation of motion for both the Kerr model [81–83] and the Schlögl model [25,84,85] in [76].
[81] P. D. Drummond and D. F. Walls, J. Phys. A **13**, 725 (1980).
[82] W. Casteels, R. Fazio, and C. Ciuti, Phys. Rev. A **95**, 012128 (2017).
[83] X. H. H. Zhang and H. U. Baranger, Phys. Rev. A **103**, 033711 (2021).
[84] F. Schlögl, Z. Phys. **253**, 147 (1972).
[85] M. Vellela and H. Qian, J. R. Soc. Interface **6**, 925 (2008).
[86] C. Jarzynski, Phys. Rev. Lett. **78**, 2690 (1997).
[87] K. Sekimoto, *Stochastic Energetics*, Vol. 799 (Springer Berlin Heidelberg, Heidelberg, 2010).